Molecular Dynamics Simulations of Freezing Behavior of Pure Water and 14% Water-NaCl Mixture Using the Coarse-Grained Model

Fatemi, Seyed Mahmood; Foroutan, Masumeh*+

Department of Physical Chemistry, School of Chemistry, University of Tehran, Tehran, I.R. IRAN

ABSTRACT: *We performed molecular dynamics simulations using the coarse-grained model to study the freezing behavior of pure water and 14% water-salt mixture in a wide range of temperatures for a very long time around 50 nanoseconds. For the salty water, an interface in nanoscale was used. For both systems, the freezing behavior of water molecules was studied using some qualities such as density, total energy, and radial distribution function. For the 14% water-salt mixture, the equilibrium freezing temperature depression observed in the simulations was well consistent with the experimental data. Contrary to the water-salt mixture, however, the above-mentioned quantities changed dramatically for the pure water at the freezing point. The plots of the total energy versus time shows the freezing point of 14% water-salt mixture was 265 K that is 9 K less than the freezing point of pure water. The reduction of freezing point is in very good agreement with the experimental freezing point. The results of the simulation showed that in the less temperature than obtained freezing point, the sodium and chloride ions tendency to network formation and rejection of solution lead to reduction of water molecules accumulation.*

KEY WORDS: *Coarse-grained model; Nanoscale; Freezing point; Pure water; 14% Water-salt mixture.*

INTRODUCTION

Water is the most utilized solvent in experimental and computational studies [1-10] particularly for biological systems. The presence of salts significantly modifies the properties of pure water, and also affects the properties of biological molecules in water [11,12]. Experimental studies of both thermodynamic and kinetic aspects of the equilibrium between salts and their saturated solutions are also crucial in geological studies [13]. Sodium chloride is one of the most abundant salts available on earth, and for this reason many experimental studies have been devoted to determining the properties of NaCl solutions, and the effect of NaCl on biological molecules [14]. It is clear that computer simulations can complement these studies by supplying a molecular perspective of the behavior of the system. For this reason, some simulation studies have been devoted to NaCl solutions [15,16] and primitive models of ionic systems [17]. The chemical potential of ions in solution has been calculated in many simulation

* *To whom correspondence should be addressed.*
+ *E-mail: foroutan@khayam.ut.ac.ir*
1021-9986/16/1/1 10/$/3.10

studies [18]. However, it is somewhat surprising to realize that the number of studies devoted to determine from molecular simulations the solubility of salts in water is quite small. *Ferrario et al.* [19] have determined for the first time the solubility of KF in water using computer simulations. Later on, *Vega et al.* [20] and *Maginn et al.* [21], and quite recently *Lisal et al.* [22] have studied the solubility of NaCl in water. *Yethiraj et al.* have used a Molecular Dynamics (MD) simulation to investigate the effect of NaCl salt on the melting of ice [23]. The difference between the freezing temperature obtained from experiment and their simulation results is about 3 K for 2m solutions. With the help of computer simulation [20,24] , *Vega et al.* have explored the solubility of NaCl in water using different force fields and they demonstrated that the solubility of NaCl in water depends on the ion-ion, water-ion and water-water interactions. Also, brine rejection from freezing salt solutions, has been studied both theoretically [24,36] and experimentally [27]. The effect of NaCl on the water-water radial distribution function as a function of salt concentration was investigated by *Soper et al.* [28]. They showed that the ion-induced perturbation to the structure of water proceeds beyond the first hydration shell. Their study emphasized the longer ranged ion-induced perturbation and related contraction of the second and third coordination shells of water molecules, while the first neighbor shell largely remains unchanged. The dissociation of NaCl in water has been studied using ab initio MD simulations [29].

In the present work, we have using a developed coarse-grained model of water [30] for studying the freezing behavior of water molecules in pure water and 14% water-salt mixture.

COMPUTATIONAL METHODS

In this work, the coarse-grained models of water and NaCl in water were used for MD simulation, where a monoatomic model of water (mW) has been used as a computational basis [28]. In an attempt to avoid challenging electrostatics in term of computational methods, ions were modeled without charge [31]. The full details of the coarse-grained models of water and NaCl in water were given in the mentioned Refs. [30] and [31], respectively.

Coarse-grain simulation model and force fields

Recently, *Molinero et al.* have developed a coarse-grained model of water that can reproduce the energy, density and structure of liquid water and its anomalies and phase transitions [31]. The force field used for the coarse-grain simulations described in this reference is the *Stillinger-Weber* (SW) [32] potential. Its form is given as:

$$E = \sum_{i}\sum_{j>i}\varphi_2\left(r_{ij}\right) + \sum_{i}\sum_{j\neq i}\sum_{k>j}\varphi_3\left(r_{ij}, r_{ik}, \theta_{ijk}\right) \quad (1)$$

$$\varphi_2\left(r_{ij}\right) = A\varepsilon_{ij}\left[B\left(\frac{\sigma_{ij}}{r_{ij}}\right)^p - \left(\frac{\sigma_{ij}}{r_{ij}}\right)^q\right]\exp\left(\frac{\sigma_{ij}}{r_{ij}a_{ij}\sigma_{ij}}\right)^p$$

$$\varphi_3\left(r_{ij}, r_{ik}, \theta_{ijk}\right) = \lambda_{ijk}\ \ \varepsilon_{ijk}\left[\cos\theta_{ijk} - \cos\theta_{0ijk}\right]^2 \times$$

$$\left(\frac{\gamma\sigma_{ij}}{r_{ij} - a_{ij}\sigma_{ij}}\right)\exp\left(\frac{\gamma\sigma_{ij}}{r_{ik} - a_{ik}\sigma_{ik}}\right)$$

For the mW-ion model, the parameters *A*, *B*, *p*, *q*, *a*, θ_0, and γ in Eq. (1) remain fixed for all pairs and triplets of interactions with the values A = 7.049556277, B = 0.602224558, p = 4, q = 0, a = 1.8, θ_0=109.48°, and γ= 1.2. The forces calculated using the SW potential between pairs and triplets vanish at the cutoff distance of r_c=1.8σ. In the mW-ion model, for the interaction between ions of the same sign a shielded Coulomb potential [33] has been added. The Yukawa potential has the form:

$$E = Ar^{-1}\exp\left(-Kr\right)\ ,\ \ r < r_c \quad (2)$$

For the attraction of Na-Cl pairs, the SW potential remains to describe the interaction. The values of the parameters for the mW and mW-ion models using the SW potential were given in Table 1. Three-body parameters for configurations ijk are the same as ikj. Terms not listed in the table (e.g., three-body terms for the triplets of ions) do not contribute to the energy.

Simulation details

The LAMMPS [34] MD package was used to equilibrate the molecules and run the simulations under NPT conditions at different temperatures and 1 atm. The pressure and temperature were controlled using a Nose-Hoover barostat and thermostat with damping parameters 500×10^{-6} nanosecond and 100×10^{-6} nanosecond, respectively.

Table 1: Force field parameters of the mW and mW-ion model [31].

Pair parameters for Eq. (1)[a]					
I	j	ε_{ij} (kcal/mol)	σ_{ij} (Å)	α_{ij}	
mW	mW	6.189	2.3925	1.8	
mW	Na	16.00	1.85	1.8	
mW	Cl	15.00	2.60	1.8	
Na	Cl	10.2	2.00	1.8	
Pair parameter for Eq. (2)					
I	j	A(kcal/mol)	κ(Å $^{-1}$)	rc	
Na	Na	1107	1.8	7.0	
Cl	Cl	1107	1.8	7.0	
Three-body parameters for Eq. (1)[b]					
I	j	K	ε_{ijk}	λ_{ijk}	Cos(θ_{0ijk})
mW	mW	mW	6.189	23.15	-1/3
mW	mW	Na	16	7	-1/3
mW	mW	Cl	15	16	-1/3
mW	Na	Na	16	7	-1/3
mW	Na	Cl	18.2	1	-1/3
mW	Cl	Cl	15	16	-1/3
Na	mW	mW	16	7	-1/3
Na	mW	Na	16	7	-1/3
Na	mW	Cl	18.2	1	0.74606
Cl	mW	mW	15	16	-1/3
Cl	mW	Na	18.2	1	0.87648
Cl	mW	Cl	15	16	-1/3

(a) Two-body parameters A = 7.049 556 277, B = 0.602 224 558, p = 4, q = 0, and γ = 1.2 same for all ij pairs interacting through the SW potential [Eq. (1)]. [b] *is the center atom, with θ_0 forming the angle between legs r_{ij} and r_{ik} (ε_{ijk} are in units of kcal/mol).*

All simulations were performed with periodic boundary (PPP) conditions. The equations of motion were integrated using the velocity Verlet algorithm with a time step of 10×10^{-6} nanosecond. Simulation boxes with dimensions of about 2.0×2.2×5.4 nanomete^3 and 10.4×2.1×2.1 nanomete^3 used for pure water and water-salt mixture, respectively. All simulations were performed for 50 nanoseconds. Long production runs were used to determine with high accuracy the different quantities of pure water and 14% NaCl solution. The initial configurations for the pure water simulations had 1584 water molecules in the liquid phase. An interface in nono scale was used for the simulation of salt-water mixture. As the study results in the next section show, the temperature of 274 K has been identified as the freezing temperature of pure water. To study the freezing behavior of pure water, we chose a wide range of temperatures. The initial configuration of the salt water mixture had 1584 water molecules in the liquid phase. The Na and Cl were initially placed by removing 144 water molecules in the middle and nanoscale distance of the cell (see Fig. 1), resulting in a solution concentration of %14. It has been shown that a system with 1584 total molecules is satisfactory for the study of ice growth [35].

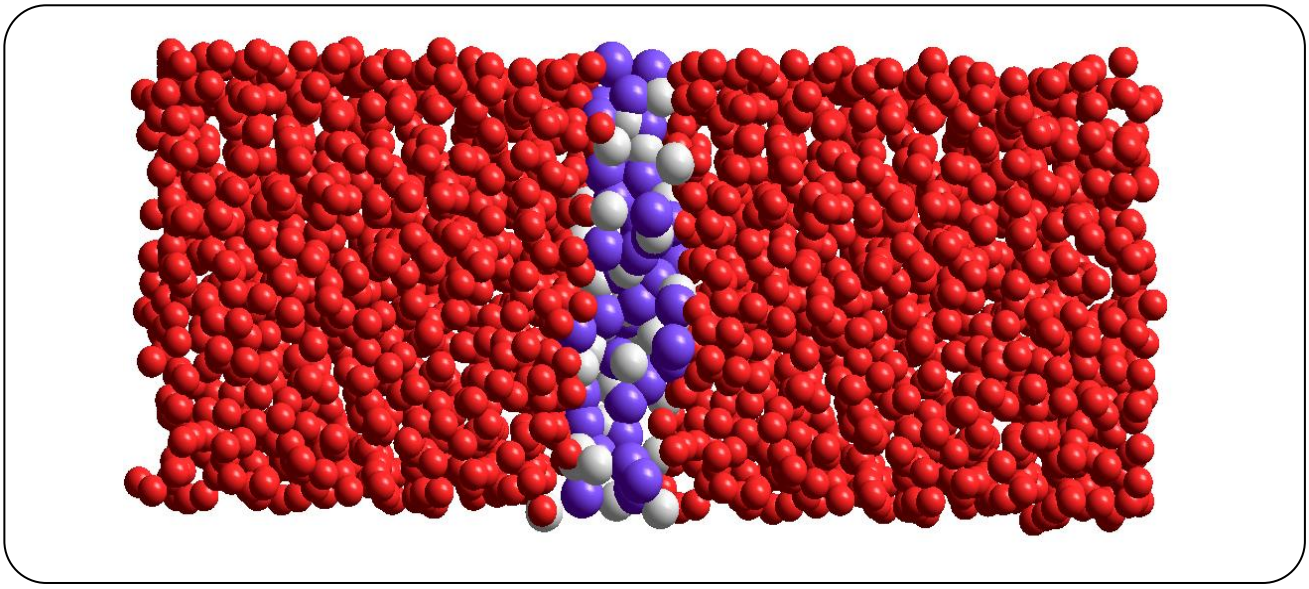

Fig. 1: The Snapshot of initial configuration of 14% water-salt mixture, The Na and Cl were initially placed in the middle and nano scale of the cell (Colors assigned to each molecule: red, water; white, Cl & purple, Na).

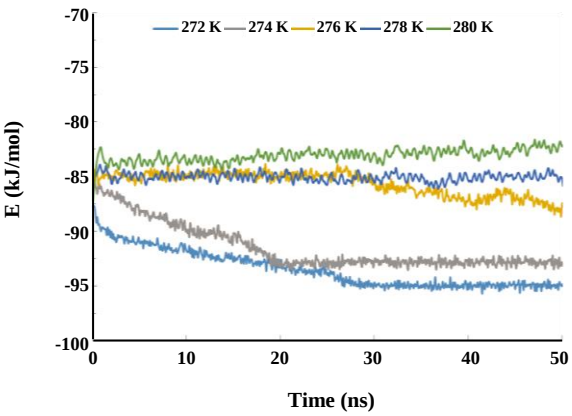

Fig. 2: The total energy vs. simulation time step of the pure water at different temperatures.

RESULTS AND DISCUSSION

In this section, we present the results of MD simulations of freezing behavior of water molecules in pure water and 14% water-salt mixture. Some time-dependent qualities like density, total energy, are used for the study of the freezing behavior of both systems. Also, Radial Distribution Functions (RDF) are provided for further understanding of freezing behavior of water molecules in both systems. This section has three subsections. In first and second subsections, the freezing behaviors of pure water and 14% water-NaCl mixture were determined, respectively. In this subsection, the salt effects on the freezing behavior of water molecules were investigated.

Study of freezing behavior of pure water

Total energy changes in pure water

According to the recent paper of *Vega* [36] in order to determine the freezing point of pure water, the total energy vs. time was calculated and shown in Fig. 2. Fig. 2 shows total energy changes vs. time of pure water for several temperatures close to water freezing temperature. The highest temperature which the system starts to freeze, i.e. 274 K, is considered as freezing point of pure water.

Density changes in pure water

The density changes vs. temperature was calculated and shown in Fig. 3a. Also, the density values obtained from SPC, TIP3P, TIP4P models [37] and experimental values [38] were given in Fig. 3b. Although for most of the studied temperatures in this work, there weren't any calculated or experimental values, the obtained values look reasonable. There is an excellent agreement between our calculated values and experimental data for density of pure water at 273 K and 276 K. Table 2 shows the freezing point and the densities of ice I_h at p=1 bar obtained from different models. As the table shows, the freezing point of pure water is a sensitive function of the employed potential. The table illustrates that there is an overall agreement between our obtained freezing point of water and the experimental value.

Table 2: Freezing point and the density of ice I_h at p=1 bar for different models.

Model	SPC	SPC/E	TIP4P	TIP4P/Ew	TIP5P	TIP4P/Ice	Coarse grain[a]	Expt.
Tm(K)	190.5	215.0	232.0	245.5	273.9	272.2	274.15	273.15
□(g/cm^3)	0.991	1.011	1.002	0.992	0.987	0.985	1.00087	0.999

(a) Present work

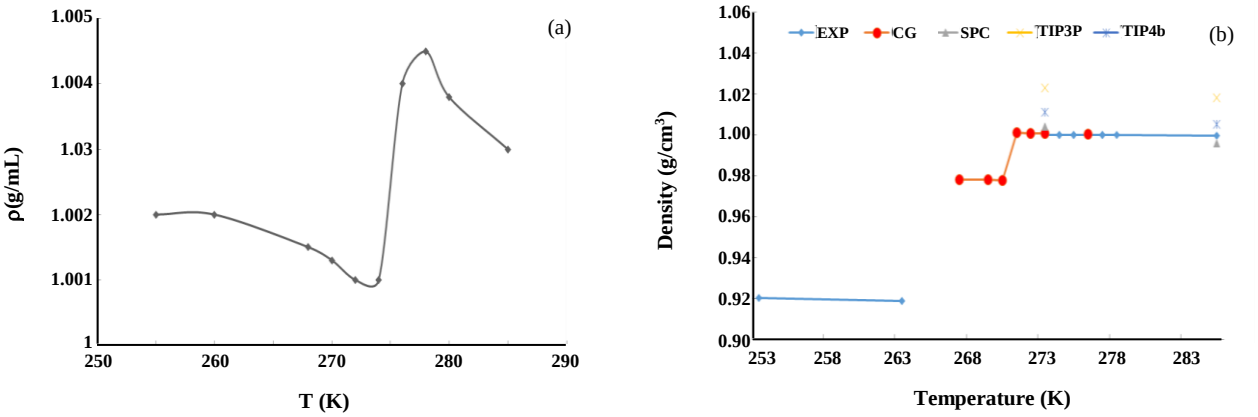

Fig. 3: (a) The density of pure water changes vs. temperature, (b) The density values obtained from SPC, TIP3P, TIP4P models and experimental values.

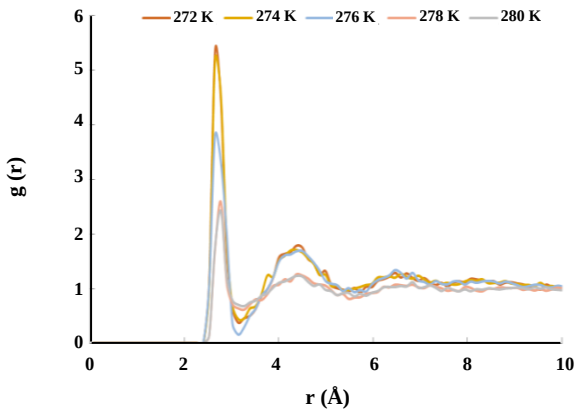

Fig. 4: RDFs for water-water.

Radial distribution functions of pure water

Fig. 4 shows the RDFs for water-water at several temperatures. As the figure shows there are sharp peaks around 2.64×10^{-1} nanometer for all temperatures. Height of the peaks was increased by decreasing the temperature.

Study of freezing temperature of 14% water-NaCl mixture

In this section, we examined the coarse-grain model for determining the freezing point of 14% water-salt mixture. Fig. 5 shows the snapshots for water-salt mixture at the final configuration at temperature 275 K.

Total energy changes of water-salt mixture at different temperatures

Fig. 6 shows the total energy changes of water-salt mixture at 260, 263, 265, 268, 270, and 272 K. As can be observed in Fig. 6, at 260, 263 and 265 K, the amount of energy was reduced over time before reaching equilibrium. So at these temperatures, system is lower than the freezing point. The constant energy of the system at 268, 270 and 272 K showed that the primary system maintained its liquid state. Therefore, 265 K (maximum temperature at which some part of the liquid is converted into ice) can be introduced as the freezing point of 14% water- NaCl mixture, Experimental calculations demonstrated this value as 266 K. Comparison of this diagram, with diagrams related to energy of pure water in Fig. 2 represents that, in the presence of salt, freezing and formation of ice crystals would occur at very long time and low temperature. So, salt causes reduction in the growth of ice crystals and speed of water freezing.

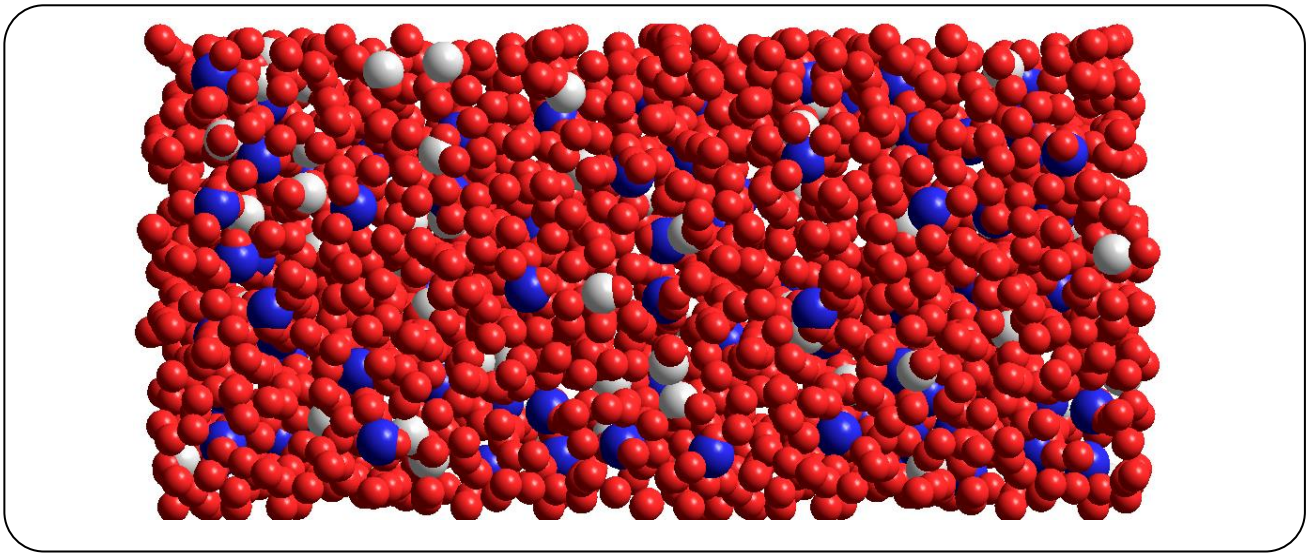

Fig. 5: Snapshots for water-salt mixture at the final configuration at temperature 275 K. (Colors assigned to each molecule: red, water; white, Cl & purple, Na).

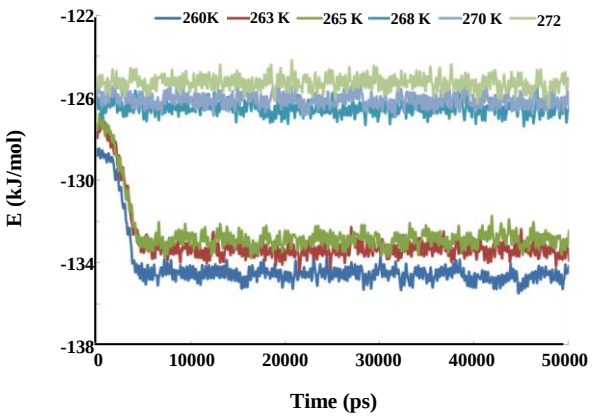

Fig. 6: Total energies of water-salt mixture at several temperatures.

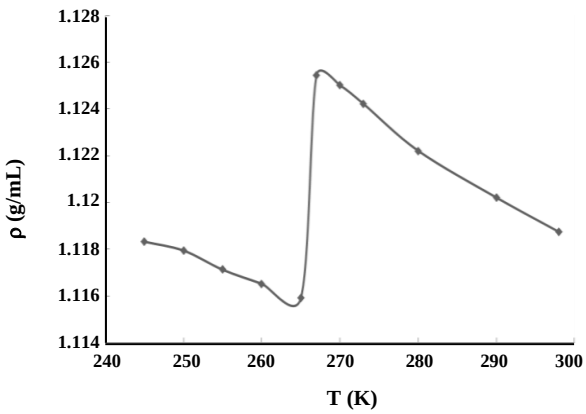

Fig. 7: The density changes vs. temperature for 14% water-NaCl mixture.

Density changes vs. temperature in water-salt mixture

According to Fig. 7 which shows the density changes vs. temperature, the simulations give a freezing point of 265 K for 14% water-NaCl mixture. As can be observed in Fig. 7, with decreasing temperature, the system density increased; however, in this curve, a sudden density reduction was observed in the system which was caused by increased volume of the system during water freezing. Table 3 shows the freezing point and the density obtained from the results of the present work compared to their experimental values and show a good agreement between the results. Similar to other force fields [38], the predicted freezing point by the coarse grain model is lower than its experimental values.

Radial distribution functions of water- NaCl mixture

In order to address the question of what happens for the sodium particles, we presented the RDFs of water-chloride and water-sodium in Fig. 8. Figs. 8(a), (b) and (c) show the water-water, water-sodium and water-chloride RDFs for water- NaCl mixture at different temperatures, respectively. The comparison of Fig. 8b and 8c shows that the height of RDF of water-sodium is more than that of water-chloride. This means that since more water molecules are around the sodium particle, we expect that sodium's role in cluster formation is lower than that for chloride.

Figs. 8 (a) shows the RDFs of water-water for water-NaCl mixture at different temperatures. As can be

Table 3: Freezing/point and density of 14% water-NaCl mixture.

Property	Experimental value	Coarse-grain model[a]
Freezing point (K)	263.21	265
Density (g/cm^3)	1.1008	1.11593

(a) Results of the present work

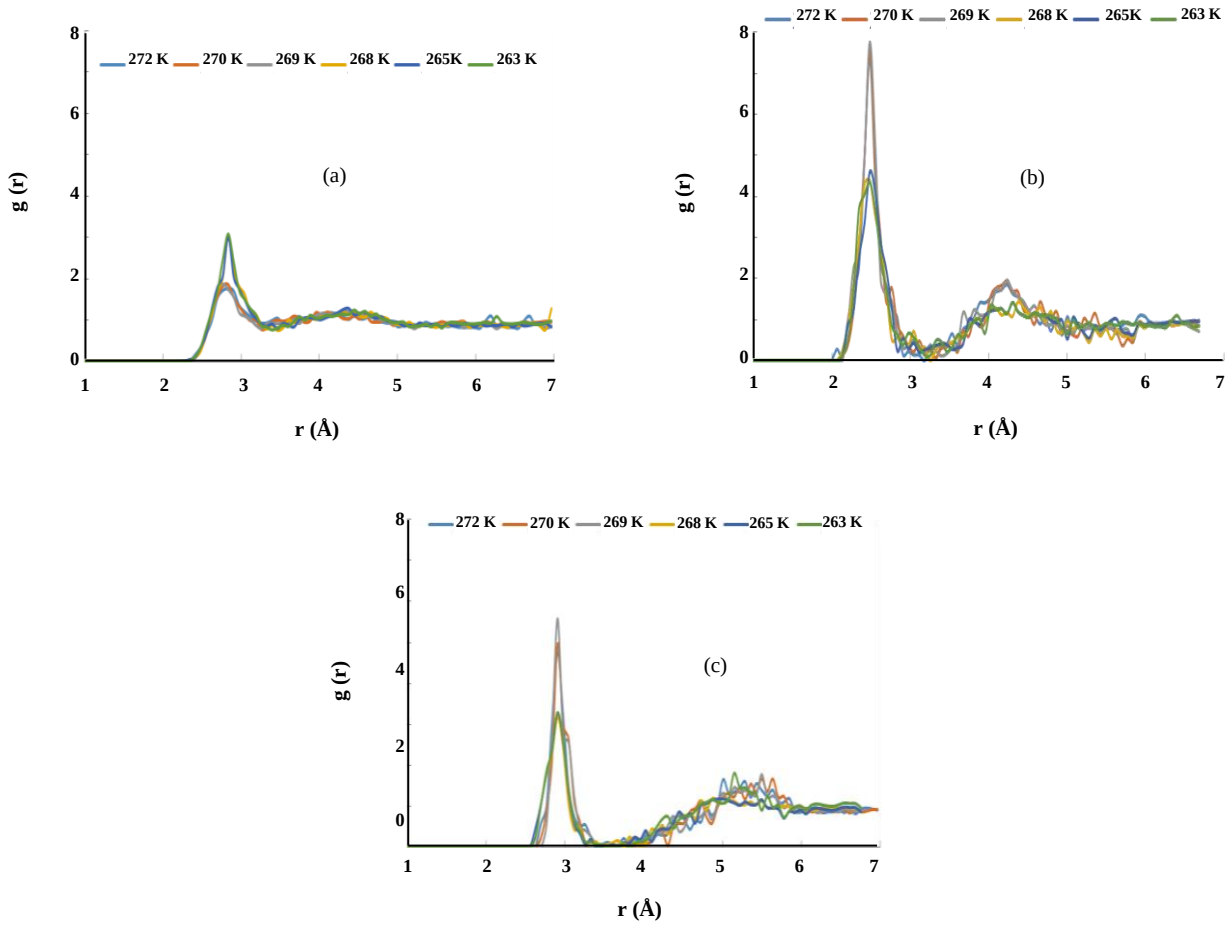

Fig. 8: (a) the water-water, (b) water-sodium and (c) water-chloride RDFs for water- NaCl mixture at different temperatures, respectively.

observed, in all the diagrams, there is always a sharp peak at a distance of 2.67×10^{-1} nanometer. These peaks show a different height for temperatures above and below the freezing point, so that, with decreased temperatures, height of the peaks would increase. These observations show that, with decreased temperature and freezing of a part of water, more assembly of water molecules occurs. Figs. 8 (b) and (c) show the RDFs of water- sodium and water-chloride for water-NaCl mixture at different temperatures, respectively. As can be detected, with temperature decrease, height of the peaks would reduce, which represent a considerable decrease in the assembly of sodium and chlorine ions around water molecules. Nor height of the peaks in oxygen-sodium RDF curve relative to oxygen-chlorine was demonstrated more assembly of sodium ions around central water molecules. Moreover, the first assembly of chlorine ions around water molecules was at a distance of 2.9×10^{-1} nanometer, while this distance was 2.48×10^{-1} nanometer for sodium ions. Less radius of sodium ions compared with chlorine provided the possibility for sodium ions to gather at a less distance than water molecules. From the RDF graphs,

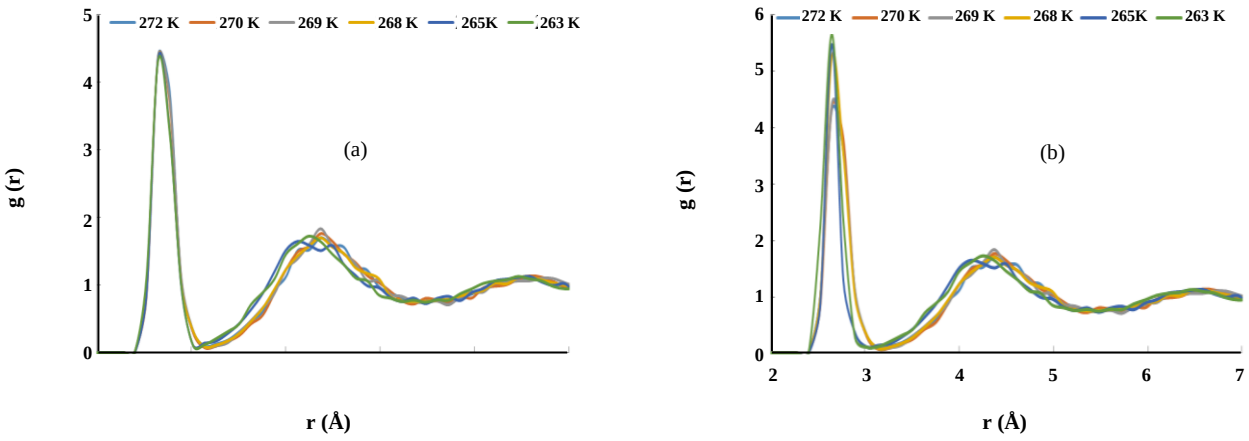

Fig. 9: RDFs of sodium- chloride (a) at the beginning of the simulation (b) at the end of simulation.

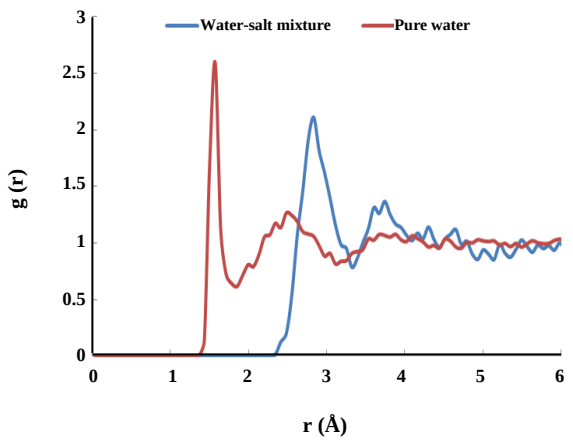

Fig. 10: Comparing of RDF for oxygen atoms in pure water and water-salt mixture.

can be understood that in the less temperature than obtained freezing point the sodium and chloride ions tendency to network formation and rejection of solution lead to reduction of water molecules accumulation. Fig. 9 shows the RDFs of sodium- chloride (a) at the beginning of the simulation (b) at the end of the simulation. In all of these diagrams, a sharp peak can be observed in 2.64×10^{-1} nanometer. The height of these peaks was identical at the beginning of simulation at different temperatures when no ice was formed yet. However, at longer times, it was observed that the height of the peaks increased by reducing temperature toward freezing point, which indicates more assembly of ions at temperatures below the freezing point.

Salt effects on the freezing behavior of water molecules in water-salt mixtures

Fig. 10 shows the comparison of RDF for oxygen atoms in pure water and water-salt mixture. Comparing RDF of oxygen atoms in pure water and salt water showed that the presence of salt led to a change in the peak height and also displacement in the first distance of water molecules. More tendencies of sodium and chlorine ions for the interaction with water molecules could reduce the correlation between water molecules. In the presence of salt, freezing point of water reduced from 270 to 265 K.

CONCLUSIONS

In this study, 50 nanosecond simulations for the freezing of water molecules in pure water and 14% water-salt mixture was performed using the coarse-grain model. For constructing the input of the simulation of salty water, an interface in nanoscale distance was used. The comparison of the obtained results for pure water and water-salt mixture shows how salt, as an anti-freezing agent, can make important changes in freezing behavior of water. Using plots of the total energy versus time, 265 K was determined as the freezing point of 14% water-salt mixture which is 9 K below the freezing point of pure water. In the less temperature than obtained freezing point the sodium and chloride ions tendency to network formation and rejection of solution lead to reduction of water molecules accumulation. Investigations showed that the correlation between water molecules was higher

at low temperatures, at which crystalline structures of ice were not formed. Comparison of oxygen-oxygen RDF of salt and water solution demonstrated that in the presence of salt, a gathering of water molecules was reduced. Comparison of chlorine-sodium RDFs at different temperatures represented that with decreased temperature, the gathering of these ions around each other increased.

Received : Apr. 22, 2014 ; Accepted : Sep. 28, 2015

REFERENCES

[1] Bahar S., Zakerian R., Ionic Liquid Based Dispersive Liquid-Liquid Microextraction and Enhanced Determination of the Palladium in Water, Soil and Vegetable Samples by FAAS, *Iran. J. Chem. Chem. Eng. (IJCCE)*, **33**: 51-58 (2014).

[2] Chamsaz M., Poor Zaryabi M.H., Arbab Zavar M.H., Darroudi A., Dispersive Liquid-Liquid Microextraction Based on Solidification of Floating Organic Drop Combined with Flame Atomic Absorption Spectrometry for Preconcentration and Determination of Thallium(III) in Water Samples, *Iran. J. Chem. Chem. Eng. (IJCCE)*, **33**: 59-66 (2014).

[3] Baradajee G.R., Mohamadi A., Efficient and Practical Protocol for the Synthesis of Pyridopyrazines, Pyrazines and Quinoxalines Catalyzed by $La(OAc)_3$ in Water, *Iran. J. Chem. Chem. Eng. (IJCCE)*, **32**: 61-67 (2013).

[4] Jamaloei B.Y., Kharrat R., The Performance Evaluation of Viscous-Modified Surfactant Water Flooding in Heavy Oil Reservoirs at Varying Salinity of Injected Polymer-Contained Surfactant Solution, *Iran. J. Chem. Chem. Eng. (IJCCE)*, **31**: 99-111 (2012).

[5] Daraei A., Treatment of Textile Waste Water with Organoclay, *Iran. J. Chem. Chem. Eng. (IJCCE)*, **32**: 67-70 (2013).

[6] Berijani S., Ahmadi G., Ultrasound Assisted Surfactant Enhanced Emulsification Microextraction and Spectrofluorimetry for Determination of Oxadiazon in Agricultural Water Samples, *Iran. J. Chem. Chem. Eng. (IJCCE)*, **33**: 41-49 (2014).

[7] Xu H., Liu D.D., He L., Liu N., Ning G., Adsorption of Copper(II) from an Wastewater Effluent of Electroplating Industry by Poly(ethyleneimine)-Functionalized Silica, *Iran. J. Chem. Chem. Eng. (IJCCE)*, **34**: 73-81 (2015).

[8] Fatemi Sh S.M., and Foroutan M., Study on Formation of Unstable Clathrate-like Water Molecules at Freezing/Melting Temperatures of Water and Salty Water, *Fluid Phase Equilib.*, **384**: 73-81 (2014).

[9] Fatemi S.M., Foroutan M., Study of Dispersion of Boron Nitride Nanotubes by Triton X-100 Surfactant using Molecular Dynamics Simulations, *J. Chem. Theory Comput.*, **13**: 1450063-1450078 (2014).

[10] Fatemi S.M., Foroutan M., Study of Dispersion of Carbon Nanotubes by Triton X-100 Surfactant using Molecular Dynamics Simulation, *J. Iran Chem. Soc.*,**12***:* 1905-1913 (2015).

[11] Bowman J.C., Lenz T.K., Hud N.V., Williams L.D., Cations in Charge: Magnesium ions in RNA Folding and Catalysis, *Curr. Opin. Struct. Biol.*, **22**: 262- 272 (2012).

[12] Allnér O., Nilsson L., Villa A., Magnesium Ion–Water Coordination and Exchange in Biomolecular Simulations, *J. Chem. Theory Comput.*, **8**: 1493-1502 (2012).

[13] Zhang F., Wang G., Kamai T., Chen W., Zhang D., Yang J., Undrained Shear Behavior of Loess Saturated with Different Concentrations of Sodium Chloride Solution, *Eng. Geol.*, **155**: 69-79 (2013).

[14] Kleinewietfeld M., Manzel A., Titze J., Kvakan H., Yosef N., Linker R.A., Muller D.N., Hafler D.A., Sodium Chloride Drives Autoimmune Disease by the Induction of Pathogenic T_H17 Cells, *Nature*, **496**: 518-522 (2013).

[15] Corradini D., Rovere M., Gallo P., Structural Properties of High and Low Density Water in a Supercooled Aqueous Solution of Salt, *J. Phys. Chem. B*, **115**: 1461-1468 (2011).

[16] Argyris D., Cole D.R., Striolo A., Ion-Specific Effects under Confinement: The Role of Interfacial Water, *ACS Nano*, **4**: 2035-2042 (2010).

[17] Vincze J., Valisko M., Boda D., The Nonmonotonic Concentration Dependence of the Mean Activity Coefficient of Electrolytes is a Result of a Balance between Solvation and Ion-Ion Correlations, *J. Chem. Phys.*, **133**: 154507-512 (2010).

[18] Zhao Y., Li H., Zeng X.C., First-Principles Molecular Dynamics Simulation of Atmospherically Relevant Anion Solvation in Supercooled Water Droplet, *J. Am. Chem. Soc.*, **135**: 15549-15558 (2013).

[19] Ferrario M., Ciccotti G., Spohr E., Cartailler T., and Turq P., Solubility of KF in Water by Molecular Dynamics using the Kirkwood Integration Method, *J. Chem. Phys.* **117**, 4947- 4953 (2002).

[20] Sanz E., and Vega C., Solubility of KF and NaCl in Water by Molecular Simulation, *J. Chem. Phys.* **126**: 014507-519 (2007).

[21] Paluch S., Jayaraman S., Shah J.K., Maginn E.J., A Method for Computing the Solubility Limit of Solids: Application to Sodium Chloride in Water and Alcohols, *J. Chem. Phys.* **133**: 124504-13 (2010).

[22] Moucka F., Lisal M., Skvor J., Jirsak J., Nezbeda I., Smith W., Molecular Simulation of Aqueous Electrolyte Solubility. 2. Osmotic Ensemble Monte Carlo Methodology for Free Energy and Solubility Calculations and Application to NaCl, *J. Phys. Chem. B,* **115**: 7849-7861 (2011).

[23] Soo J., Yethiraj A., The Effect of Salt on the Melting of Ice: A Molecular Dynamics Simulation Study, *J. Chem. Phys.* **129**: 124504-12 (2008).

[24] Aragones J.L., Sanz E., Vega C., Solubility of NaCl in Water by Molecular Simulation Revisited, *J. Phys. Chem.* **136**, 244508-16 (2012).

[25] Vrbka L., Jungwirth P., Brine Rejection from Freezing salt Solutions: A Molecular Dynamics Study, *Phys. Rev. Lett.,* **95**: 148501-504 (2005).

[26] Kim D.H., A review of Desalting Process Techniques and Economic Analysis of the Recovery of Salts from Retentates, *Desalination*, **270**: 1-8 (2011).

[27] Nagashima K., Furukawa Y., Time Development of a Solute Diffusion Field and Morphological Instability on a Planar Interface in the Directional Growth of Ice Crystals, *J. Cryst. Growth*, **209**: 167-174 (2000).

[28] Mancinelli R., Botti A., Bruni F., Ricci M.A., Soper A.K., Perturbation of Water Structure Due to Monovalent Ions in Solution, *Phys. Chem. Chem. Phys.*, **9**: 2959-2967 (2007).

[29] Timko J., Bucher D., Kuyucak S., Dissociation of NaCl in Water from ab Initio Molecular Dynamics Simulations, *J. Chem. Phys.*, **132**: 114510-18 (2010).

[30] Moliero V., Moore E., Water Modeled as An Intermediate Element between Carbon and Silicon, *J. Phys. Chem. B,* **113**: 4008-4016 (2009).

[31] DeMille R.C., Molinero V., Coarse-Grained Ions Without Charges: Reproducing the Solvation Structure of NaCl in Water Using Short-Ranged Potentials, *J. Chem. Phys.* **131**, 034107-16 (2009).

[32] Stillinger F.H., Weber T.A., Computer Simulation of Local Order in Condensed Phases of Silicon, *Phys. Rev. B,* **31**: 5262-5271 (1985).

[33] Carre A. Berthier L. Horbach J. Ispas S., Kob W., Amorphous Silica Modeled with Truncated and Screened Coulomb Interactions: A Molecular Dynamics Simulation Study, *J. Chem. Phys.,* **127**: 114512-20 (2007).

[34] Plimpton S., Fast Parallel Algorithms for Short-Range Molecular-Dynamics. *J. Comput. Phys.,* **117**: 1-19 (1995).

[35] Garignano M.A., Shepson P.B., Szleifer J., Molecular Dynamics Simulations of Ice Growth from Supercooled Water., *Mol. Phys.* **103**: 2957-2967 (2005).

[36] Fernández R.G., Abascal J.L.F., F Vega C., The Melting Point of Ice Ih for Common Water Models Calculated from Direct Coexistence of the Solid-Liquid Interface, *J. Chem. Phys.* **124**: 144506-11 (2006).

[37] Jorgensen W.L., Jenson C., Temperature Dependence of TIP3P, SPC, and TIP4P Water from NPT Monte Carlo Simulations: Seeking Temperatures of Maximum Density, *J. Comput. Chem.* **19**: 1179-1186 (1998).

[38] Lide D.R., "CRC Handbook of Chemistry and Physics" (86th ed.), Boca Raton (FL): CRC Press (2005).